

Secretion and membrane recycling in plant cells: novel intermediary structures visualized in ultrarapidly frozen sycamore and carrot suspension-culture cells

L.A. Staehelin and R.L. Chapman*

Department of Molecular, Cellular and Developmental Biology, Box 347, University of Colorado, Boulder, CO 80309, USA

Abstract. Freeze-fracture electron microscopy of propane-jet-frozen samples has been employed to investigate vesicle-mediated secretion and membrane recycling events in carrot (*Daucus carota* L.) and sycamore maple (*Acer pseudoplatanus* L.) suspension-culture cells. Stabilization of the cells by means of ultrarapid freezing has enabled us to preserve the cells in a turgid state and to visualize new intermediate membrane configurations related to these events. Indeed, many of the observed membrane configurations, such as flattened membrane vesicles with slit-shaped membrane fusion sites and horseshoe-shaped membrane infoldings, appear to result from the action of turgor forces on the plasma membrane. Individual cells exhibited great variations in numbers and types of membrane configurations postulated to be related to secretion and membrane-recycling events. In the majority of cells, the different membrane profiles displayed a patchy distribution, and within each patch the membrane configurations tended to be of the same stage. This result indicates that secretory events are triggered in domains measuring from 0.1 to about 10 μm in diameter. Based on an extensive analysis of the different membrane configurations seen in our samples, we have formulated the following model of vesicle-mediated secretion in plant cells: Fusion of a secretory vesicle with the plasma membrane leads to the formation of a single, narrow-necked pore that increases in diameter up to about 60 nm. During discharge, the vesicle is flattened, forming a disc-shaped structure perpendicular to the plane of the plasma membrane. As the vesicle is flattened, the pore is con-

verted to a slit, the maximum length of which coincides with the diameter of the flattened vesicle. The flattened vesicle then tips over and concomitantly the plasma-membrane slit becomes curved into a horseshoe-shaped configuration as it extends along the outer margins of the tipped-over vesicle. Some coated pits are present interspersed between the above-mentioned structures, but their numbers appear insufficient to account for an exclusively endocytotic mechanism of membrane recycling. Instead, our micrographs are more consistent with a mixed mode of recycling of membrane components to the cortical endoplasmic reticulum and to Golgi cisternae that involves both internalization of membrane by endocytosis and of individual lipid molecules by unknown mechanisms (lipid exchange proteins?). To this end, overall flattening out of the horseshoe-shaped membrane infoldings is accompanied by a retraction and reduction in size of their central, tongue-like structure.

Key words: *Acer* – *Daucus* – Cell culture – Freeze-fracture (rapid freezing) – Membrane recycling – Plasma membrane – Secretion (vesicle-mediated).

* Present address: Department of Botany, Louisiana State University, Baton Rouge, LA 70803, USA

Abbreviations: ER = endoplasmic reticulum; PF = protoplasmic face of a freeze-fractured membrane; EF = exoplasmic (endoplasmic) face of a freeze-fractured membrane

Introduction

Vesicle-mediated secretion is an important mechanism for transferring cytoplasmically synthesized substances to the exterior of both plant (Mollenhauser and Morré 1980; Robinson and Kristen 1982) and animal (Farquhar 1985) cells. In the case of secretory glycoproteins, this process involves synthesis of precursor forms in the rough endoplasmic reticulum (ER), processing in the Golgi apparatus, packaging into secretory vesicles, and transfer to and secretion at the cell surface. Since secretion involves fusion of the vesicle membrane

with the plasma membrane, excess membrane has to be recycled from the cell surface to the appropriate internal membrane compartment.

During the past decade, detailed information on secretion and membrane recycling in animal and yeast cells has been obtained (Farquhar 1985; Schekman 1985). Secretion from plant cells has received less attention, with most studies focussing on the role of ER and Golgi apparatus in the synthesis and processing of secretory (and storage) molecules (Morré et al. 1979; Robinson and Kristen 1982; Chrispeels 1983; Robinson 1984). Few recent studies have been devoted to the actual secretory events (Volkman 1981; Kroh and Knui-man 1985) or to membrane recycling in plant cells (Kristen and Lockhausen 1983; Morré and Molenhauser 1983; Picton and Steer 1983; Joachim and Robinson 1984; Tanchak et al. 1984). It has been generally assumed that the mechanisms found in animal cells also apply for plant cells but it has been noted that normal plant cells show few if any endocytotic membrane configurations (reviewed by Robinson and Kristen 1982).

Because of the rapidity of many of the membrane changes associated with exocytosis (0.1–10 ms), only advanced cryofixation techniques can provide the temporal resolution needed to capture transient events for electron-microscopical analysis. Not only do chemical fixatives stabilize membranes orders of magnitude slower than the best ultrarapid freezing techniques (Gilkey and Staehelin 1986), but they also rapidly increase the permeability of membranes to Ca^{2+} , thereby inducing further exocytotic events during fixation (Plattner 1978). This means that all studies in which membrane changes associated with exocytotic events have been examined in chemically fixed cells are of questionable value. For example, during the past ten years, numerous publications have reported that both in animal and plant cells clearing of membrane particles and formation of a pentalaminar diaphragm occurs at the presumptive fusion site just prior to exocytosis (Lawson et al. 1977; Orci et al. 1977; Orci and Perrelet 1978; Aunis et al. 1979; Volkman 1981, 1984). However, careful analysis of micrographs of exocytotic events in ultrarapidly frozen neuromuscular junctions (Heuser et al. 1979), mast cells (Chandler and Heuser 1980), *Limulus* amoebocytes (Ornberg and Reese 1981), and adrenal chromaffin cells (Schmidt et al. 1983) have failed to confirm the particle-clearing hypothesis. Instead, membrane fusion was shown in all instances to start as a focal event without prior rearrangements of intramembrane particles.

Recycling of membrane components from the cell surface to the Golgi apparatus by means of coated pits and vesicles has been well documented in a variety of animal cell systems (Fisher and Rebhun 1983; Steinman et al. 1983; Farquhar 1985). Recent studies of plants have shown that coated pits and vesicles are capable of endocytosing cationized ferritin in protoplasts of bean leaf and soybean suspension-culture cells (Joachim and Robinson 1984; Tanchak et al. 1984) and heavy-metal salt solutions in walled cells (Hübner et al. 1985). However, the importance of coated pits and vesicles for plasma-membrane recycling is difficult to assess because of the absence of information on the rates of the uptake processes observed. Further complicating the issue are observations indicating that coated vesicles and pits may also be involved in transporting materials from the Golgi apparatus to the cell surface (Nakamura and Miki-Hiroshige 1982; Robertson and Lyttleton 1982; Griffing et al. 1986).

In this study we have used ultrarapid freezing techniques in conjunction with freeze-fracture electron microscopy to study dynamic membrane events associated with secretion and-or membrane recycling in sycamore-maple and carrot suspension-culture cells. Suspension-culture cells and not intact tissues were chosen for this investigation because propane-jet freezing only allows vitrification of biological samples with a thickness of less than 40 μm . However, more recently we have succeeded in preserving cells of intact pea roots by high-pressure freezing and have been able to confirm the unique membrane configurations reported here (Craig and Staehelin 1986).

Materials and methods

Cultures. Initial cultures of wild carrot (*Daucus carota* L.) cells were kindly provided by W.F. Boss, North Carolina State University, Raleigh, USA. Later experiments were performed with cells derived from carrot suspension cultures (*D. carota* L. culture No. 3301A) given to us by Agrigenetics, Inc. (Boulder, Colo. USA). Both types of cultures were grown in B5 medium (Gamborg 1982) containing 1 or 2 mg/l 2,4-dichlorophenoxyacetic acid (2,4-D). Cultures were maintained at 25° C on a rotary shaker (approx. 120 rpm) in the dark or under continuous low light, and subcultured every 7 d. Suspension cultures of sycamore-maple cells (*Acer pseudoplatanus* L.) were obtained from P. Albersheim, University of Colorado, Boulder. These cells were grown under standard conditions as described by Talmadge et al. (1973).

Freeze-fracture. Cells in their logarithmic phase of growth were harvested 18 h to 7 d after subculturing. In early experiments this was done by centrifugation at 1000 rpm with a Sorvall (Sorvall Instruments, Newtown, Conn., USA) GLC-2B tabletop centrifuge or at 60 rpm with a hand-cranked centrifuge.

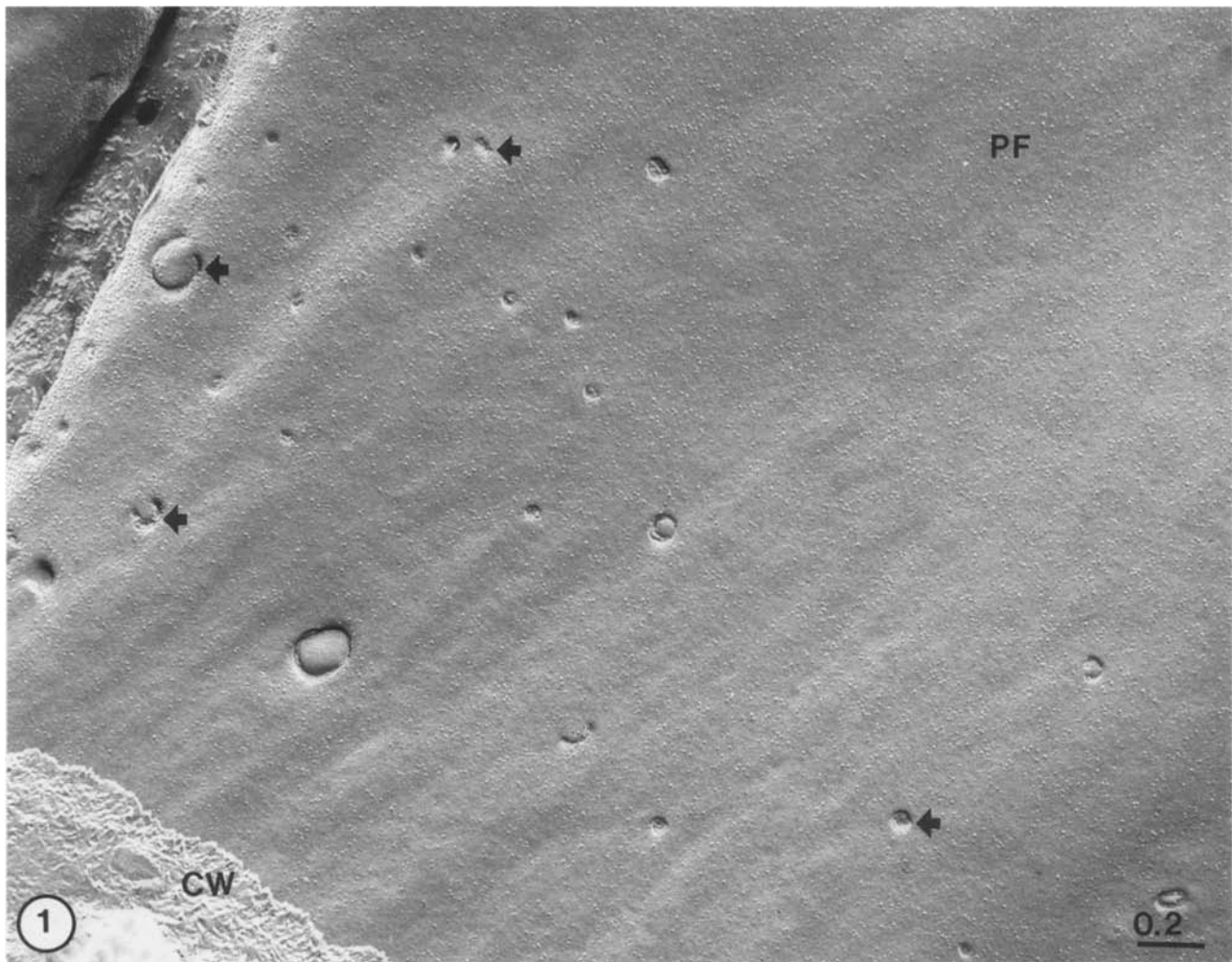


Fig. 1. Overview freeze-fracture micrograph of a propane-jet-frozen carrot suspension-culture cell. Note the smooth, turgid appearance of the plasma membrane (PF view), which attests to the quality of freezing, and the patchy distribution of the secretory membrane configurations (*arrows*). *CW* = cell wall. $\times 45000$. Magnification bar(s) here and in all micrographs = $0.2 \mu\text{m}$

In later studies we used a $63\text{-}\mu\text{m}$ Nitex (Small Parts Inc., Miami, Fla., USA) mesh to concentrate cells suspended in a Petri dish quickly immediately before transfer to a specimen holder and freezing.

Cells were collected for freezing by dipping a gold slot grid ($30 \mu\text{m}$ thick) into the concentrated suspension. The grid was then mounted between two hollowed out (0.13 mm thick in center) gold double-replica supports (Balzers High Vacuum Corp., Hudson, N.H., USA) and ultrarapidly frozen by liquid propane (-188°C) sprayed from two sides in a propane-jet freezer (Gilkey and Staehelin 1986). Double replicas were produced at -107°C in a Balzers BA 360 freeze-etch device and were cleaned in full-strength commercial bleach (approx. 5.25% NaOCl) at room temperature overnight, 70% sulfuric acid at 60°C for 45 min, and 0.25 M chromic acid at room temperature for 2 h (Platt-Aloia and Thomson 1982). Replicas were unfolded (when necessary) with 1:1 (v/v) chloroform:methanol at room temperature (1 min). The membrane fracture faces are labeled according to Branton et al. (1975).

Thin sectioning. Sycamore suspension-culture cells were fixed in 2.5% glutaraldehyde in 50 mM cacodylate buffer, $\text{pH } 7.2$, for 2 h (fixative added at room temperature and samples then

placed on ice). Following four buffer washes over 1 h, the cells were fixed in 2% OsO_4 in the same buffer (1 h at 2°C). After three cold-water washes the samples were dehydrated in a graded series of ethanol and propylene oxide, and embedded in Spurr's resin (Polysciences, Warrington, Pa. USA). Sections were poststained with 2% uranyl acetate in 1:1 (v/v) water-methanol (10 min) and with triple lead stain (2 min; Sato 1968).

Results

General appearance of the plasma membrane. Freeze-fracture micrographs of well-preserved, ultrarapidly-frozen carrot and sycamore suspension-culture cells reveal large expanses of turgid plasma membrane interrupted in many instances by variable numbers of attached vesicular structures (Figs. 1–9). A typical example of a carrot cell exhibiting a smooth turgid plasma membrane with unevenly distributed vesicular profiles is shown in Fig. 1. We interpret these membrane infoldings as

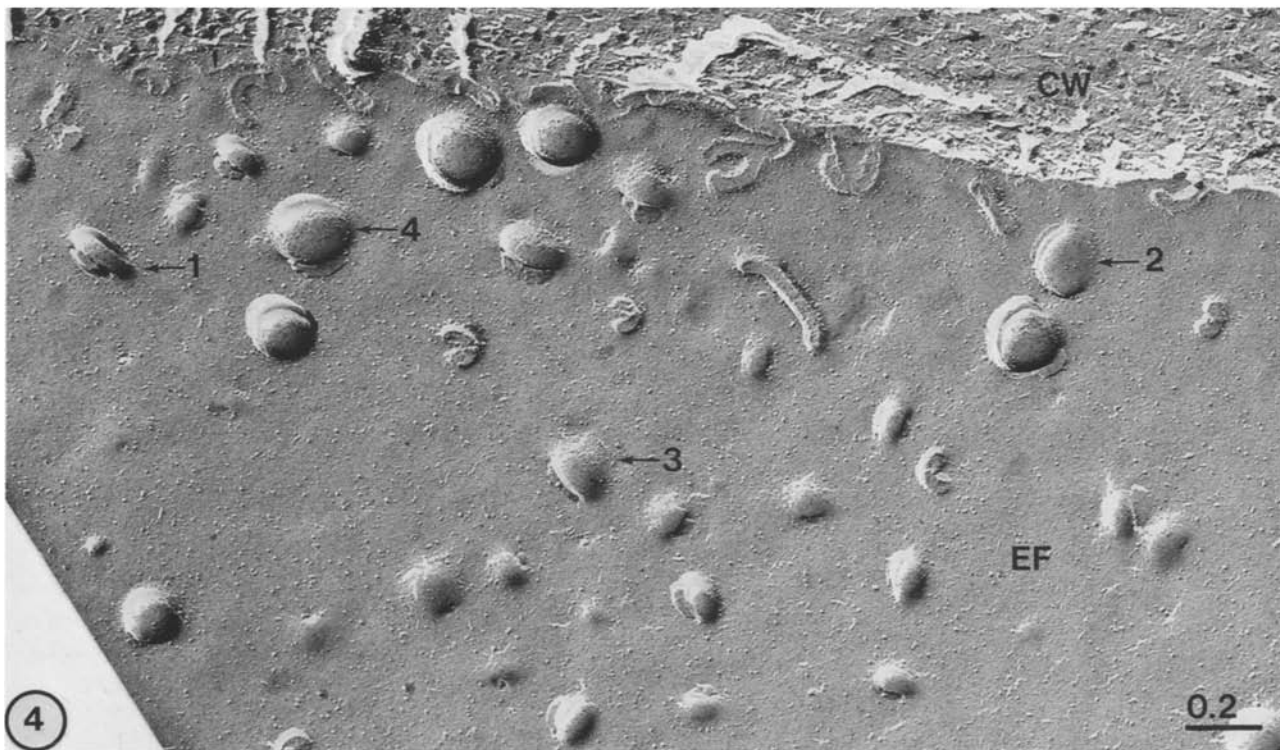
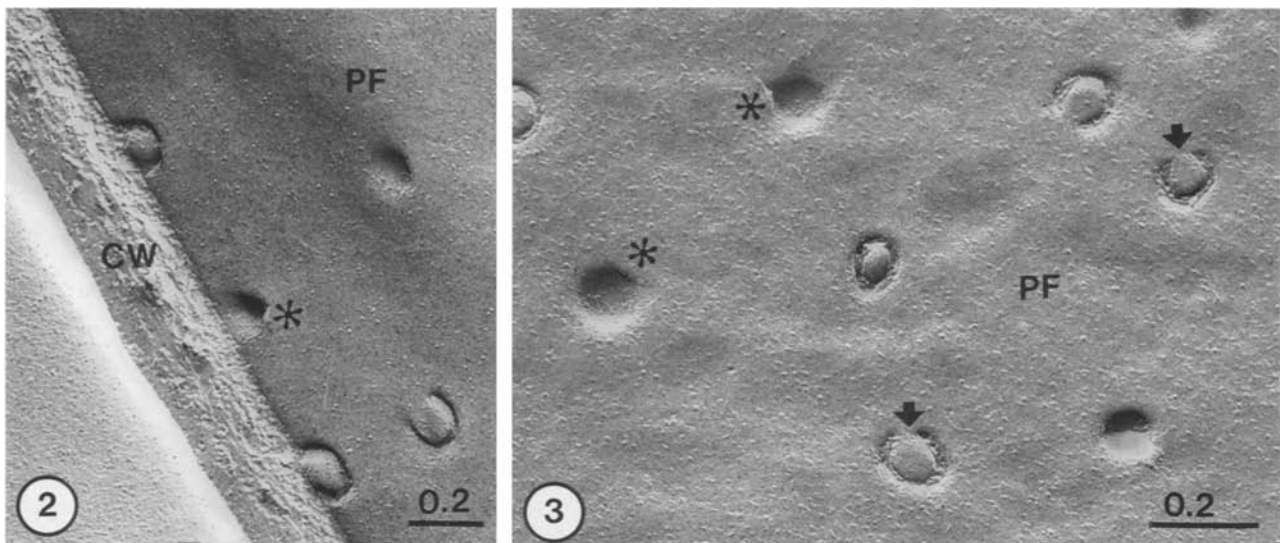


Fig. 2. P-face view of a carrot tissue-culture cell plasma membrane illustrating the spatial relationship between horseshoe-shaped membrane configurations and the cell wall (CW). The asterisk denotes a stub on the rim of a round depression; similar stubs are seen in Fig. 3 and explained in the diagram Fig. 15. $\times 50000$

Fig. 3. Micrograph of a carrot cell depicting two different PF views of horseshoe-shaped membrane infoldings. A round depression is formed when the fracture plane passes along the bottom (cytoplasmic side) of the membrane infolding and the "tongue" is broken away, giving rise to a stub (asterisks) on one side of the depression (B-type fracture, Fig. 15). Horseshoe-shaped structures are seen where the fracture remains in the plane of the plasma membrane adjacent to the cell wall (A-type fracture, Fig. 15). The arrows point to the attachment sites of the tongue-shaped membrane folds which give rise to the stubs marked by the asterisks. $\times 70000$

Fig. 4. E-face view of the plasma membrane of a sycamore-maple cell showing a large number of secretory structures. This plasma membrane is somewhat unusual in that it exhibits a great diversity of different membrane configurations in a small area. The arrows labeled 1-4 denote a postulated sequence of membrane changes associated with the tipping over of a flattened vesicle (see diagram, Fig. 16, Stages III and IV). Arrow No. 1 marks a flattened vesicle attached perpendicularly to the plasma membrane (Stage III), No. 2 a tipped-over flat vesicle (early Stage IV), No. 3 a tipped-over flat vesicle whose margin is fused with the plasma membrane on one side (medial Stage IV), No. 4 a tipped-over flat vesicle with fused margins extended three-quarters around (late Stage IV, see also Figs. 2, 3, 5, 6). Visualization of these intermediate structures requires fixation by means of ultrarapid freezing. $\times 50000$

different stages of vesicle secretion and-or membrane recycling bases on their general morphology and on the fact that the number of such profiles is reduced when secretion is slowed down. Often these structures are organized into patches and within each patch most profiles display similar configurations (Figs. 1–3, 5–9). However, cells exhibiting more evenly dispersed vesicle profiles or mixed populations of invaginations are also observed (Fig. 4). The synchrony of vesicle profiles in the patches indicates that secretion-triggering signals are perceived and responded to in domains varying from less than 0.5 to about 10 μm in diameter.

Horseshoe-shaped membrane configurations. The most frequently observed membrane configuration is the vesicle-fusion stage that gives rise to horseshoe-shaped profiles in the plane of the membrane (Figs. 2, 3, 5, 6, 15, 16). The same type of plasma-membrane configuration also gives rise to a round depression with a stub on its side in PF views (Figs. 2, 3), and a corresponding dome-like structure with a dimple on its side in EF views (Figs. 4, 7). As illustrated in Fig. 15, a stub on the edge of a round depression arises when the fracture plane passes along the bottom (cytoplasmic side) of a horseshoe-shaped membrane infolding and the “tongue” is broken away. If the fracture plane remains in the plane of the plasma membrane adjacent to the cell wall, horseshoe-shaped profiles result (Figs. 15, 16). The curvature and the extent of closure of the horseshoe structures is variable, ranging from an open, boomerang-like configuration to structures that form nearly closed rings (Figs. 2–7, 9). In the latter instances, the base of the membrane “tongues” can be extremely constricted (Fig. 5, insert). The overall depth of the membrane infoldings, as evidenced by the height of the the EF dome structures (Fig. 7) is related to the size of the membrane “tongues.” Shallow infoldings (Fig. 7, arrow B) have small “tongues” (Fig. 7, arrow B’) and large, deep infoldings (Fig. 7, arrow A) larger ones (Fig. 7, arrow A’).

The diameter of the dome and horseshoe-shaped membrane profiles varies from about 100 to 220 nm, with a modal peak between 140 and 160 nm. In some cells, two or more distinct size categories can often be distinguished within a given patch (Figs. 5, 6), but in most instances, the vesicle-fusion profiles of each cluster tend to be uniform in size (Figs. 3, 7). The membrane surface area within an average dome/horseshoe vesicle fusion structure is equivalent to the surface area of a vesicle with a diameter of about 110–120 nm.

Slit-like and small, round membrane infoldings. Slit-like infoldings are produced by fused vesicles that are flattened in a plane perpendicular to the plasma membrane (Figs. 4, 8, 9, 16). Such vesicles appear to represent a more transient state of the vesicle secretion/recycling process since they are seen less frequently than the horseshoe configurations. A slit-like infolding in the plasma membrane is observed (Figs. 8, 9) when the attached, flattened vesicle is fractured through its neck; in contrast, a disc-shaped structure is seen in EF views when the fracture plane passes *around* a flattened vesicle (Figs. 4, 9). Although most of the disc structures are oriented perpendicular to the plane of the membrane, some are tilted (Fig. 4, arrow No. 2). Membrane areas containing both slit-like infoldings and horseshoe-shaped profiles often display a continuum of intermediate structures, i.e., bent “slits” and wide open “horseshoes” (Figs. 4–7, 9), indicating that the two types of membrane configurations are interrelated. Slit-infolding lengths vary from 80 to 220 nm, with a modal peak at about 120 nm. The larger values coincide with the maximal diameter of plasma membrane-attached, flattened vesicles.

Plasma membrane infoldings with small, round openings (CP in Figs. 5, 6, 8) occur less frequently than the horseshoe-shaped profiles but are often interspersed with such profiles (Figs. 5, 6). Occasionally, however, a cell may exhibit a whole field of such small round invaginations (Fig. 8). While some of these profiles may represent cross-fractured neck regions of larger vesicles in the initial phase of fusion, most appear to correspond to small, round and fused vesicles with an average diameter of 60 nm (Figs. 6, 8) and which appear to be freeze-fracture equivalents of coated pits.

Several particle rosettes, postulated to be structural equivalents of cellulose-synthase complexes, are also visualized in Fig. 8. As previously reported (Chapman and Staehelin 1986), fewer rosettes are seen on plasma membranes of carrot and sycamore suspension-culture cells exhibiting numerous vesicle fusion figures. Why this is the case we do not know.

Thin-section images. In an attempt to visualize the above-described vesicle secretion/recycling structures in conventional thin sections, we have chemically fixed sycamore suspension-culture cells in a low-concentration buffer to preserve their plasma membranes in a smooth, “turgid” state. Figures 10–13 are micrographs of such chemically fixed cells. Three types of plasma-membrane infoldings can be discerned. The most distinct struc-

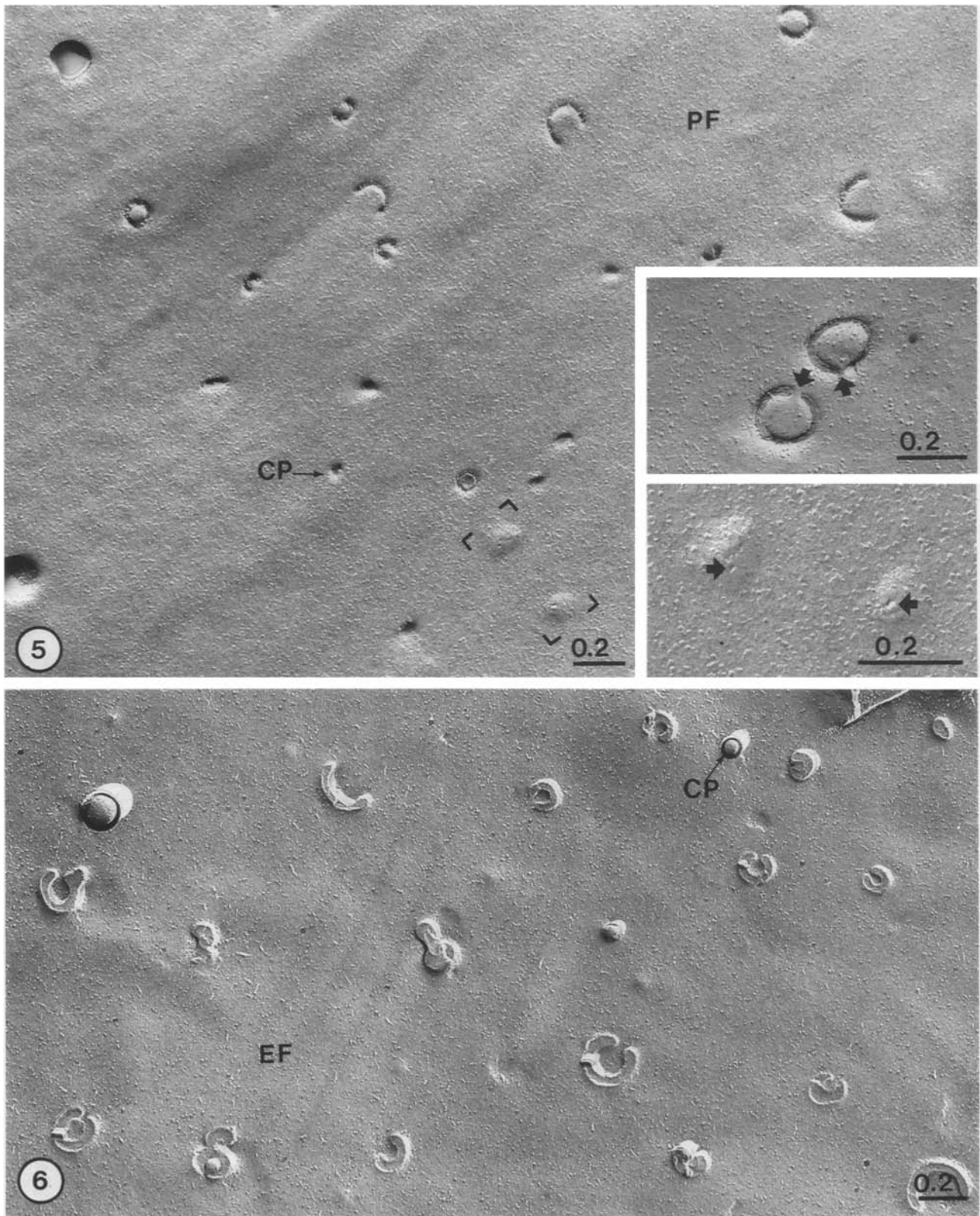


Fig. 5. Plasma-membrane PF of a carrot cell displaying horseshoe-shaped membrane infoldings of different size. We postulate that the variation in size of the “horseshoes” is the result of vesicles of different sizes fusing with the plasma membrane. Only one potential coated pit (CP) profile is evident. $\times 45000$. *Top insert:* Horseshoe-shaped structures with only tenuous connections between their membrane “tongues” and the surrounding plasma membrane. $\times 60000$. *Bottom insert:* Higher magnification of the boxed area in Fig. 5 showing two plasma-membrane bulges with small pits (*arrows*) that may represent a very early stage of vesicle fusion. $\times 90000$

Fig. 6. EF view of typical horseshoe-shaped membrane configurations of a sycamore-maple cell. As in Fig. 5, the “horseshoes” are of different sizes and reveal different degrees of closure. CP=Coated pit. $\times 40000$

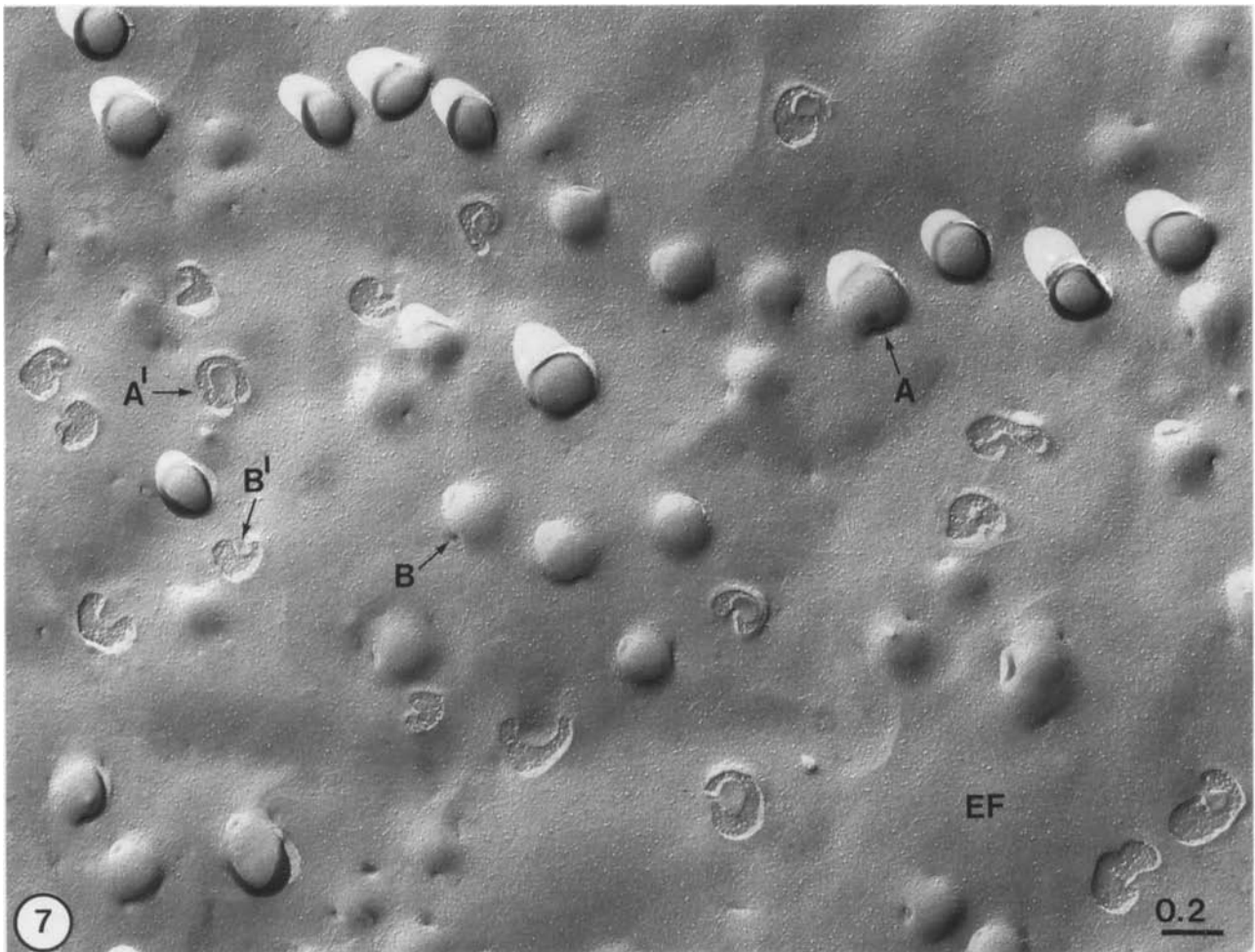


Fig. 7. Plasma-membrane EF of a sycamore-maple cell depicting numerous horseshoe-shaped/dome-shaped membrane configurations. (The dome-shaped structures are complementary to the round depression structures seen in Fig. 3 and are shown diagrammatically in Fig. 15.) Note the differences in height of the domes (A versus B types), most of which exhibit a dimple at their base. The *A'*, *B'* arrows denote the corresponding horseshoe-type membrane configurations. Note the small size of the membrane "tongues" in *B'* versus *A'* structures. The size of these membrane folds appears to decrease as the domes become flatter (see Fig. 17 for an interpretation). Domes with more than one dimple on their side correspond to overlapping horseshoe-shaped membrane infoldings. $\times 40000$

tures are pear-shaped and flattened vesicles fused with the plasma membrane (Figs. 10, 11). Less clearly defined in shape, but more frequently seen, are rounded membrane bulges (Fig. 12). On one side of such bulges the unit membrane of the plasma membrane often appears fuzzy as if a second, overlapping unit-membrane fragment were present. In addition, poorly staining vesicular structures may be discerned between the bulging plasma membrane and the cell wall (Figs. 10, 12). Since the diameter of these differentiated plasma-membrane bulges coincides with the diameter of the horseshoe/dome-shaped membrane configurations seen in freeze-fracture replicas (Figs. 2–7), it is possible that the two types of images show the same membrane structures.

Coated pits represent the third type of plasma-

membrane configuration that can be recognized in our thin sections (Fig. 13). Even though their coat elements stained only lightly, the even curvature of the small, round membrane profiles made identification possible in many instances. However, the frequency with which indentifiable coated pits were seen was rather low in all of our specimens. Based on their diameter of 40–80 nm, their shape, and the frequency with which they are seen in thin sections, we postulate that the equivalent freeze-fracture structures are the uniformly round, small dome-shaped membrane infoldings with an average diameter of about 60 nm (Figs. 5, 6, 8).

Cortical ER and vesicles. In suitably fractured cells displaying numerous secretory structures, extensive, fenestrated sheets of endoplasmic reticulum

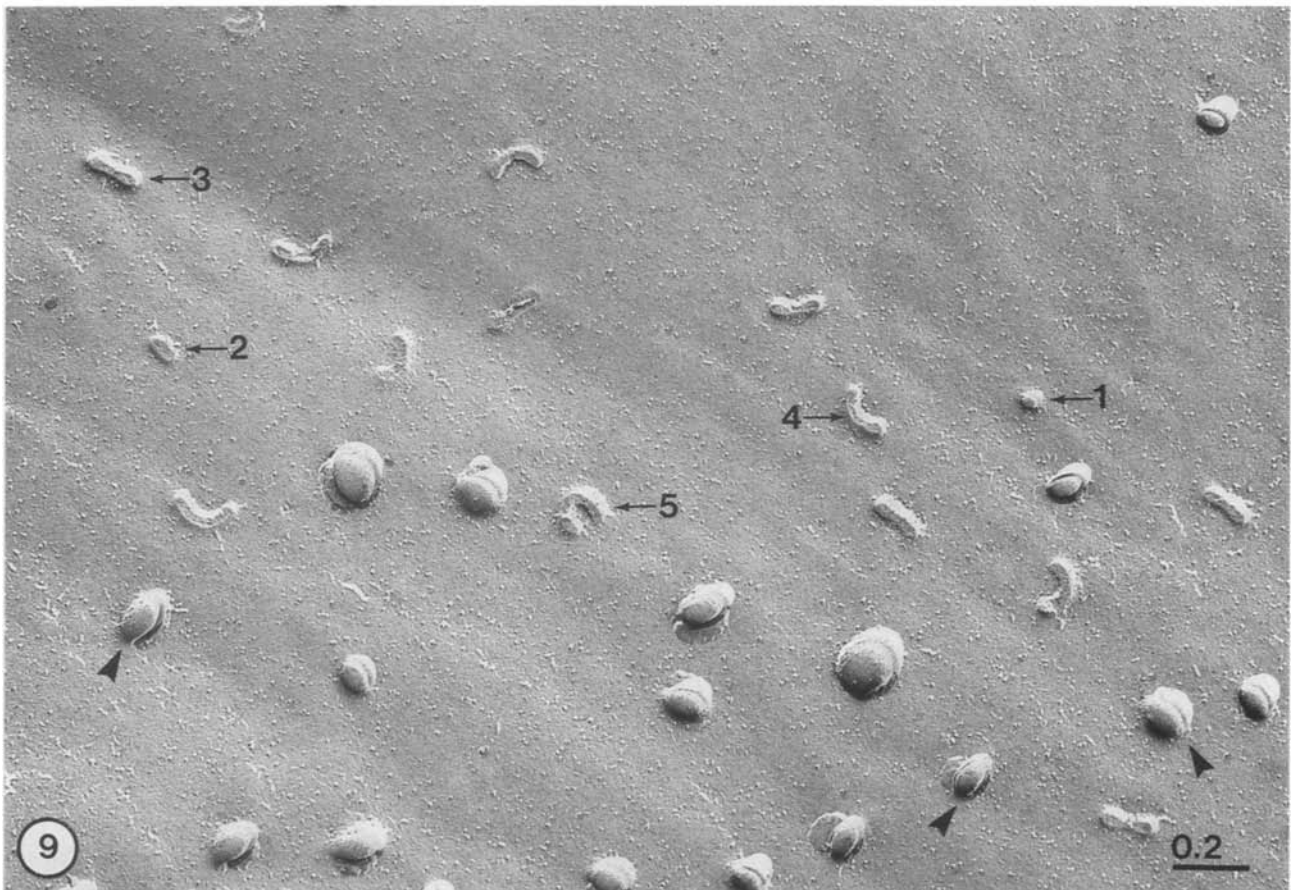
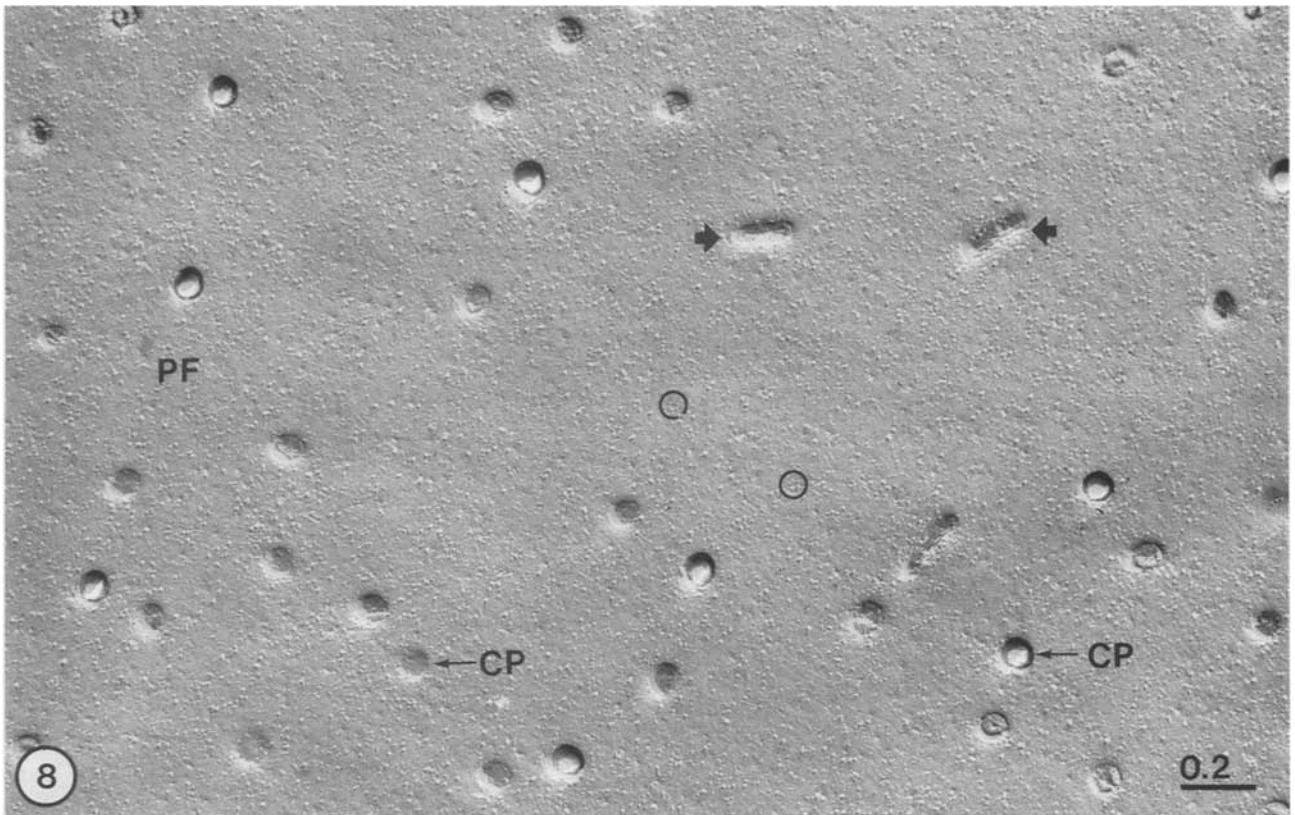


Fig. 8. Plasma membrane (P-face) of a sycamore-maple cell exhibiting both slit-like (*arrows*) and round membrane infoldings (*CP*). The former represent fusion sites of flattened vesicles with the plasma membrane (see Figs. 6, 9), the latter correspond mostly to coated pits (see Figs. 6, 13). Two particle rosettes, postulated cellulose-synthase complexes, are marked by *circles*.
 × 50000

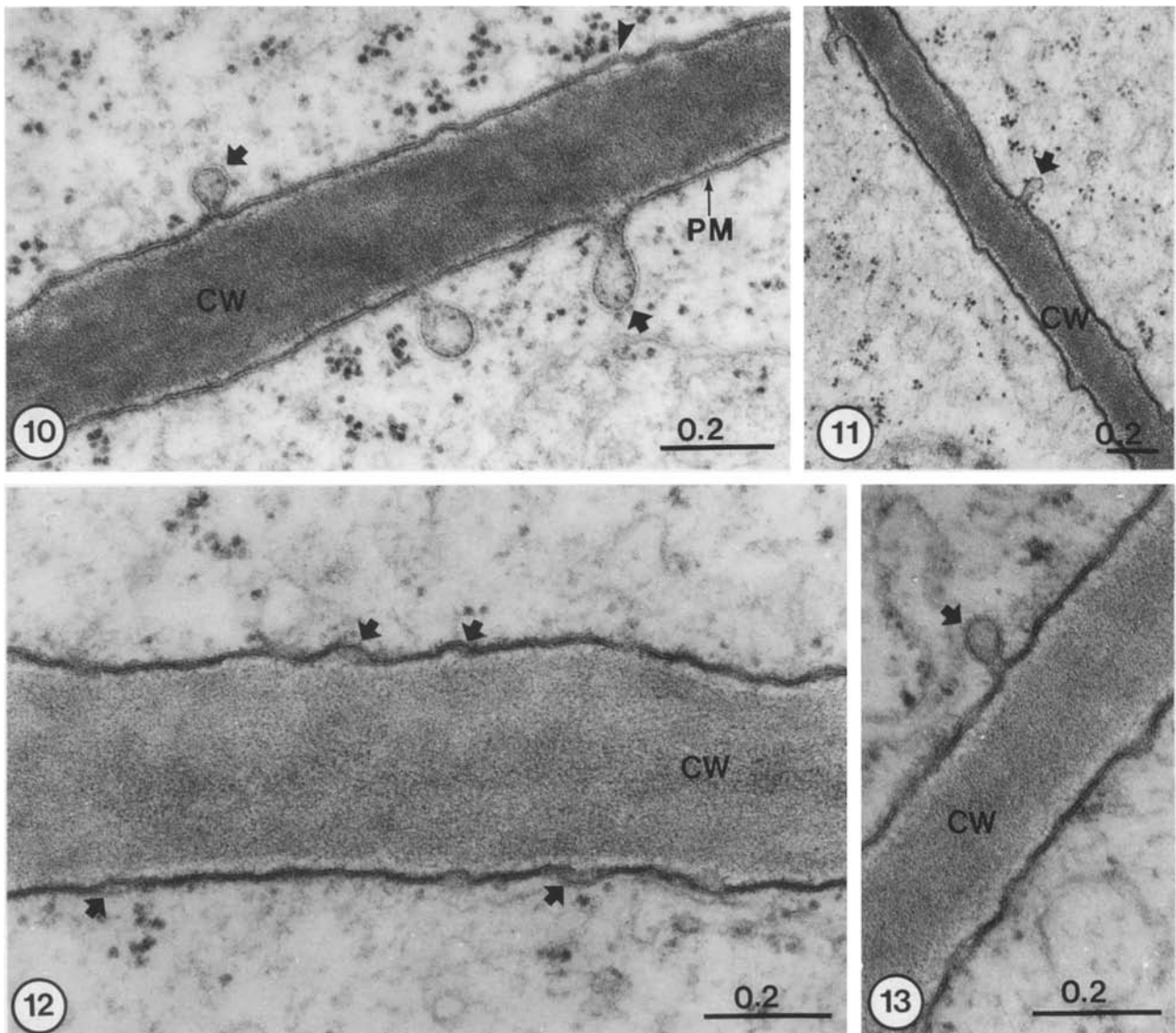


Fig. 10–13. Thin-section electron micrographs of sycamore-maple suspension-culture cell plasma-membranes (*PM*) and adjacent cell walls (*CW*)

Fig. 10. Vesicles (*arrows*) fused with adjacent plasma membranes and presumed to be involved in the discharge of their contents into the cell wall. Note the flattening of the vesicle on the right. The *arrowhead* points to a lightly staining vesicular structure external to the plasma membrane. $\times 80000$

Fig. 11. Plasma membrane with an attached flattened vesicle (compare with Figs. 4, 9). $\times 34000$

Fig. 12. Plasma membranes displaying many irregular bulges (folds) with overlapping segments of unit membranes (*arrows*). These bulges appear to correspond to tipped-over flattened vesicles that give rise to the horseshoe-shaped configurations see in Figs. 2–6 and 9. $\times 90000$

Fig. 13. Thin section image of a coated pit (*arrow*). $\times 90000$

Fig. 9. Plasma-membrane EF of a sycamore-maple cell displaying attached flattened vesicles (*arrowheads*) and several slit-like infoldings (*arrows*). The latter arise when a flattened vesicle is fractured at the level of the plasma membrane. The *arrows* labeled 1–5 indicate the postulated sequence of changes that occur as a secretory vesicle fuses with the plasma membrane and is converted into a flattened vesicle and then into a horseshoe-shaped configuration (see also Fig. 4, arrows 1–4, and Stages II–IV of Fig. 16). Straight slits are produced by flattened vesicles oriented normal to the plasma membrane, curved slits by flattened vesicles that have tipped over and make a smaller than 90° angle with the plasma membrane. $\times 50000$

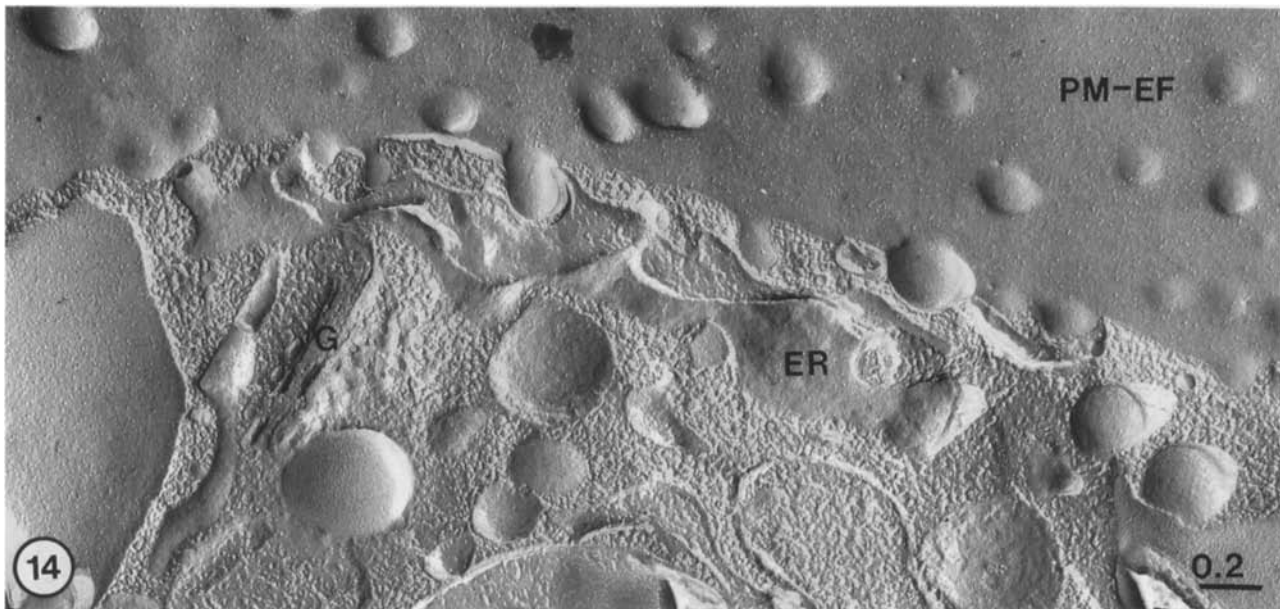


Fig. 14. Freeze-fracture micrograph of the cortical cytoplasm of a sycamore cell. Note the extensive endoplasmic reticulum (*ER*) immediately adjacent to the plasma membrane (*PM-EF*), which displays numerous secretion structures. This cortical ER system could control vesicle fusion by regulating local Ca^{2+} levels and also participate in the molecular recycling of membrane lipids (see text and Fig. 17). *G* = Golgi apparatus. $\times 40000$

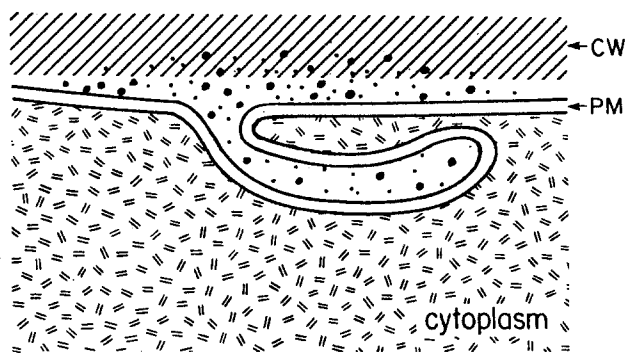
membranes are regularly observed immediately adjacent to the plasma membrane and often nearly touching the membrane infoldings (Fig. 14). However, fusion of ER membranes with the plasma membranes was never observed. Since ER membranes are known to control local calcium levels in the cytoplasm and calcium is essential for membrane fusion (Hepler 1981; Palevitz and Hodge 1984; Hepler and Wayne 1985) this peripheral ER could be instrumental in regulating the fusion of vesicles with the plasma membrane. In addition, it would be ideally positioned to participate in the molecular recycling of membrane lipids (see *Discussion*).

For unknown reasons, the number of vesicles in the cortical cytoplasm appears to be relatively low when compared to the number of plasma-membrane infoldings seen in our samples. Three explanations, not mutually exclusive, are: the transit time of a vesicle between a Golgi apparatus and the plasma membrane is short compared to the lifetime of a membrane infolding; sampling in a freeze-fracture replica image is only in the plane of the fracture, whereas in thin-section images sampling is throughout the depth of the section; chemical fixation may lead to the accumulation of vesicles in the cortical cytoplasm before all cellular movements are stopped. Although important, elucidation of these problems is beyond the scope of our investigation.

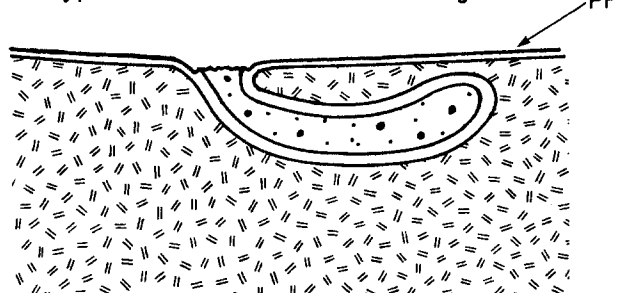
Discussion

Our current study of ultrarapidly frozen and freeze-fractured plant tissue-culture cells has led to the discovery of novel plasma-membrane structures that appear to be unique to plants and to represent intermediate stages in vesicle-mediated secretion and membrane recycling. These membrane configurations fall into three categories: flattened vesicle-type infoldings (Figs. 4, 8, 9, 11), horseshoe-shaped membrane infoldings (Figs. 2–7, 9), and small, round infoldings (Fig. 5, 6, 8). Because only rounded infoldings have been observed to date in studies of vesicle-mediated secretion and membrane recycling in both plant and animal cells, it is important to review first the validity of the new findings and then to proceed to discuss the origin, the temporal relationship, and the functional significance of the different types of membrane profiles.

Validity of the electron-microscopical images. Our findings were made possible by the use of ultrarapid freezing techniques to stabilize the cells in a completely turgid state for electron-microscopical analysis. As pointed out in the *Introduction*, only advanced cryofixation techniques (freezing of entire specimen within 5 ms) can provide the quality of freezing and the temporal resolution needed to consistently capture transient events associated



A-type fracture : horseshoe configuration



B-type fracture : rounded depression with stub

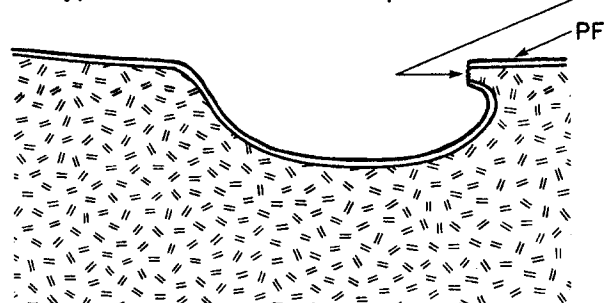


Fig. 15. Schematic diagram illustrating how a horseshoe-shaped membrane infolding (Figs. 3–7, 16) can give rise to two types of PF images (and corresponding EF images) depending on the plane of the fracture. An A-type fracture, which arises when the fracture plane remains at the level of the plasma membrane, produces horseshoe-shaped membrane profiles (Figs. 5, 6). A B-type fracture occurs when the fracture plane passes around the membrane infolding, thereby producing a large, round depression with a stub on one side in PF views (Figs. 2, 3) and a dome with a dimple on its side in EF views (Fig. 7). The PF stub corresponds to the remains of the torn-away horseshoe “tongue”. The dimples of the EF dome structures are the complementary structures of the PF stubs

with vesicle-mediated secretion; chemical fixatives are orders of magnitude too slow and may even produce artifactual membrane configurations (reviewed by Gilkey and Staehelin 1986). To ensure the validity of our observations further, we have consistently used cells from cultures during their logarithmic phase of growth, and by using a nylon

mesh to harvest the cells from a Petri dish very quickly we also ensured adequate oxygenation right up to the time of freezing. Since completing this study, we have also been able to visualize all of the membrane configurations described in this study in intact pea and corn root tips stabilized by high-pressure freezing (Craig and Staehelin 1986). For these reasons we are confident that the novel types of membrane infoldings reported here are real and not caused by the propane-jet ultrarapid freezing technique or by specimen manipulation prior to freezing.

Comparison of vesicle-mediated secretion and membrane recycling in plant and animal cells. Membrane flow associated with vesicle-mediated secretion and membrane recycling is a well-characterized phenomenon in animal cells (Farquhar 1985). The limited amount of information on plant cells indicates that the same mechanisms operate with certain modifications (Robinson and Kristen 1982). Thus, because most plant cells secrete much smaller amounts of protein, vesicle movement between ER and Golgi apparatus is considerably reduced. On the other hand, vesicle traffic between the Golgi apparatus and the plasma membrane appears to be at least as great in plant as in animal cells. Reported rates of turnover for plasma membranes vary from about 1% of surface area per minute for fibroblasts (Steinman et al. 1983) and for the alga *Pleurochrysis* (Brown et al. 1970) to 3% per minute for the gland cells of the plant *Mimulus tilingii* (Schnepf and Busch 1976), and even 9% per minute for the ovary-gland cells of the plant *Aptenia cordifolia* (Kristen and Lockhausen 1983). Thus, plant cells face the same basic problem as animal cells in terms of packaging and transporting secretory products to the cell surface and recycling excess plasma membrane back into the cytoplasm, but the exact mechanism employed have eluded characterization.

Although three recent studies have provided convincing evidence for the uptake of macromolecules by plant cells (Joachim and Robinson 1984; Tanchak et al. 1984) and of heavy-metal ions (Hübner et al. 1985) by means of endocytosis mediated by coated pits, the importance of endocytotic mechanisms for plasma-membrane recycling in plant cells remains an enigma (Robinson and Kristen 1982; Robinson 1984). Cram (1980) has postulated that pinocytosis is a very energy-inefficient, and thus improbable, mechanisms for uptake of nutrients by plant cells, since turgor-pressure forces of opposite sign have to be overcome. For this reason, consideration has been given to the

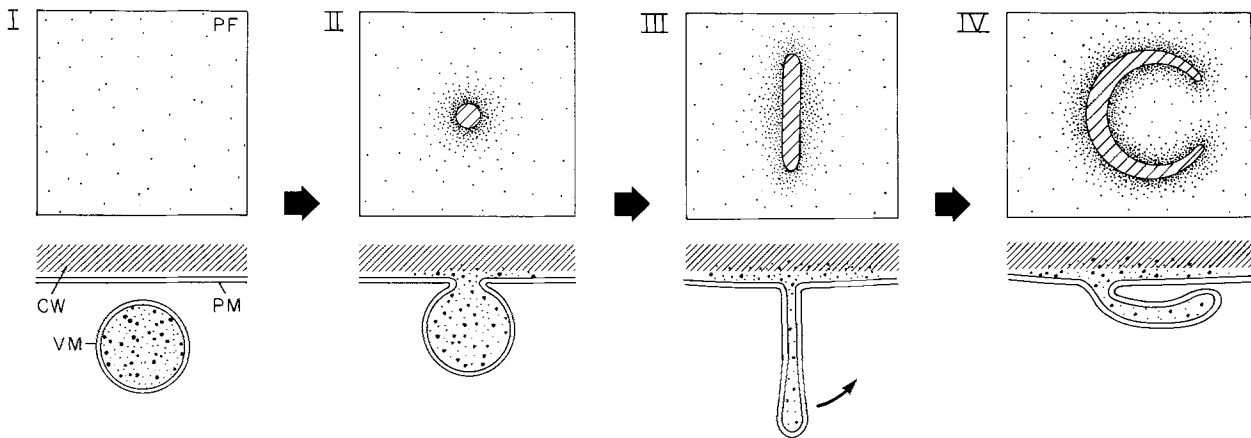


Fig. 16. Speculative diagram illustrating the proposed sequence of events associated with vesicle-mediated secretion in plant cells. The top row of diagrams depicts face-on views of the plasma membrane as observed in our freeze-fracture replicas (PF images), the lower one, cross-sectional views of the membrane-associated vesicular structures. Stages I and II: approach of a secretory vesicle to the plasma membrane (PM) and fusion of the vesicle membrane (VM) with the plasma membrane. These stages are the same as in animal cells. However, starting with Stage III, membrane configurations that seems to be unique to plants are seen. Because of the fact that plant cells are under turgor pressure and their plasma membranes cannot expand freely, the round, fused vesicle (Stage II) collapses into a discoidal structure as its contents are released (Stage III). Subsequently the membrane fusion site is deformed into a slit (Stage III, top). The flattened vesicle then tips over to form the structures shown in Stage IV. The formation of the horseshoe-shaped membrane profile (Stage IV, top) involves elongation and curving of the "slit" (Stage III) by fusion of the outer margin of the tipped-over vesicle with the plasma membrane. Stage IV is by far the most frequently seen configuration, indicating that it is also the most stable

idea of recycling of individual membrane components (lipid molecules) in contrast to whole membranes (Schnepf 1974; Robinson and Kristen 1982). No experimental observations have been published to date that would provide direct support of this hypothesis, but as discussed below, our results support it in an indirect manner.

A new model of vesicle-mediated secretion in plant cells. Cram's (1980) contention that turgor pressure severely affects the ability of plant cells to take up nutrients by pinocytosis provided the stimulus for us to think about the possible effects of turgor pressure on the mechanisms of secretion and membrane recycling in plant cells. This hypothesis has also guided us in the formulation of the models of vesicle-mediated secretion and membrane recycling illustrated in Figs. 16 and 17, which are based on an analysis of over 500 electron micrographs of ultrarapidly frozen carrot and sycamore-maple culture cells accumulated over a three-year period. During the analysis of our micrographs and the formulation of our models we have placed special emphasis on accounting for all plasma-membrane configurations reproducibly observed in our specimens. As presented, the models contain both experimentally proven facts, the different membrane configurations visualized in our samples, as well as highly speculative features, the sequences of events by which a given

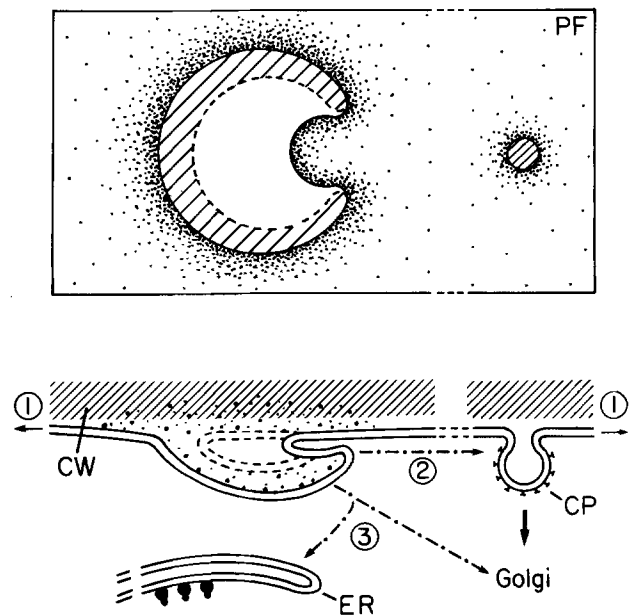


Fig. 17. Schematic diagram illustrating three possible mechanisms for removing excess membrane from a horseshoe-shaped infolding of the plasma membrane. Top diagram depicts face-on (PF) view of the plasma membrane; bottom diagram shows a cross-sectional view. *Pathway 1* depicts cell-expansion-caused withdrawal of membrane from the fold. *Pathway 2* involves lateral flow of membrane (proteins and lipids) into a forming coated vesicle that subsequently pinches off and is transferred back to the Golgi apparatus. *Pathway 3* is more hypothetical and postulates molecular recycling (most likely of lipids by means of lipid exchange proteins) from the plasma membrane to ER and Golgi membranes

membrane configuration may be related to other membrane configurations. Thus, as new information becomes available the postulated sequence of events may have to be altered, but any revised model will also have to account for all of the types of membrane configurations shown in our models. By conveying our ideas in diagrammatic form we hope to focus attention on critical structural aspects of vesicle-mediated secretion and membrane recycling in plant cells that can be and need to be experimentally verified.

The two initial events of vesicle-mediated secretion, namely, approach of a vesicle to the plasma membrane and initial fusion (Fig. 16, Stages I and II), correspond to what has been documented for ultrarapidly frozen animal cells (Heuser et al. 1979; Ornberg and Reese 1981; Plattner 1981; Schmidt et al. 1983). Thus, membrane fusion appears to start as a focal event leading to a small orifice through which the secretory molecules are ejected (Fig. 5, lower insert, Figs. 8, 9). Positive identification of initial secretion pores has not yet been possible in our samples since we have not succeeded in finding conditions for turning off and then rapidly restarting vesicle-mediated secretion in plant cells. Cooling sycamore cells to 4° C, a condition that would inhibit most endocytic processes in animal cells, had only a small effect on the number and type of membrane invaginations seen in our samples (data not shown). This finding confirms the report of Morris and Northcote (1977) that secretion of soluble polysaccharides by sycamore suspension-culture cells is only minimally affected by temperature changes in the range of 0–35° C. Lowering extracellular calcium does lead to an inhibition of polysaccharide secretion (Morris and Northcote 1977), but our preliminary observations indicate that low extracellular calcium levels may have multiple effects on membrane architecture, thus making interpretation of the changes difficult (data not shown).

Stage III of our model (Fig. 16) represents the first type of membrane configuration unique to plants. In this stage a flattened vesicle is seen fused perpendicularly to the plasma membrane, giving rise to a slit-like membrane infolding (Figs. 4, 8–11).

We propose that the formation of these flattened vesicles is a consequence of the turgid state of plant cells and the close appression of the plasma membrane against the cell wall. Thus, when a secretory vesicle fuses with the plasma membrane and discharges its contents, its membrane cannot be automatically incorporated as in animal cells because rapid expansion of the plasma membrane

cannot occur. As a result, the vesicle membrane collapses onto itself, giving rise to a flattened, disc-like membrane infolding. Shortly thereafter the round pore is converted into a slit (Fig. 9).

The transition from Stage III to Stage IV (Figs. 16) is most readily explained by the basic instability of the flattened vesicles oriented perpendicular to the plasma membrane. As soon as such a vesicle tips over (see postulated intermediate steps in Figs. 4, 9) it becomes stabilized in this new configuration as a consequence of extension of the fused margins of the flattened vesicle with the plasma membrane. This extension converts the slit-like openings to the typical horseshoe-shaped membrane infoldings illustrated in Figs. 2, 3, 5, 6, 9.

Our model (Fig. 16) makes several testable predictions. For instance, testing of the postulated sequence of events of vesicle-mediated secretion should be straightforward as soon as it becomes possible to trigger secretion in plant cells in a precise manner, as can be done in certain animal systems. Further, in the absence of turgor pressure, no *new* flattened vesicles and slit-like membrane infoldings should be formed but horseshoe configurations may persist for some time after transfer of cells to a hypertonic medium. Preliminary observations of cells treated in this manner (not shown) appear to lend support to this theory in that only horseshoe-shaped and round membrane infoldings are seen. In the case of α -amylase-secreting barley aleurone cells maintained in an essentially iso-osmotic medium, no slit-like plasma-membrane infoldings were observed in micrographs of ultrarapidly frozen cells by Fernandez and Staehelin (1985).

Mechanisms for recycling excess plasma membrane to the cytoplasm. Following the conversion of the unstable, flattened vesicle configuration to the apparently more stable horseshoe structure (Fig. 16), the stage seems to be set for removal of the membrane fold and return of the plasma membrane to a flat configuration. The abundance of the horseshoe-shaped membrane infoldings indicates that this return is a comparably slow process.

Withdrawal of membrane material from the infoldings is indicated by the presence of horseshoe-shaped membrane configurations with more flattened profiles and with tongue-shaped membrane folds of diminished size (Figs. 7, 17). However, the mechanism of this withdrawal is still unclear. It is obvious that cell expansion uses up some of the new membrane material, but where rates of cell expansion have been correlated with rates of vesicle-mediated secretion (Picton and Steer 1983),

more membrane appears to be delivered to the cell surface by vesicles than is needed for cell expansion. Thus, some recycling of membrane molecules to the cytoplasm is a must. As mentioned earlier, cationized ferritin and heavy-metal ions have been shown to be taken up into plant cells by means of coated pits (Joachim and Robinson 1984; Tanchak et al. 1984; Hübner et al. 1985). In our freeze-fracture micrographs coated pits appear as small, round membrane infoldings (Figs. 5, 6, 8) interspersed between slit- and horseshoe-shaped membrane profiles. Since the number of these small round infoldings is quite low in most cells (see Figs. 5–7; but compare with Fig. 8, which displays an unusually high density of such infoldings), it is questionable whether they can account for all of the required membrane recycling. This being the case one has to postulate that the remaining molecules must be recycled by other means, most likely as individual molecules.

It is well documented that lipid exchange proteins can mediate the transfer of individual molecules between membranes *in vitro* (Tanaka and Yamada 1979; Helmkamp 1986), and probably also *in vivo* (Kaplan and Simoni 1985). Furthermore, when a plant, an alga or a bacterium is subjected to a sudden chilling stress, individual lipid molecules are removed from its plasma membranes, the fatty-acid tails modified to adjust membrane fluidity, and finally the altered molecules returned to the membrane (Lynch and Thompson 1984). All of these studies demonstrate that individual lipid molecules can be extracted from a given membrane and that such extracted molecules may be transferred to another membrane system. In plant cells, lipid exchange proteins could mediate the transfer of excess phospholipid molecules from the plasma membrane to the ER and to the Golgi apparatus, so that they would become again available for the assembly of secretory vesicles. The close proximity of ER cisternae to plasma-membrane regions rich in different kinds of membrane infoldings (Fig. 14) could make this kind of molecular membrane recycling a very efficient process, but our micrographs do not prove that this kind of transfer is actually taking place. However, in no instance have we observed a plasma membrane to be physically continuous with the underlying ER. Further experiments are sorely needed to gain a better understanding of all of these membrane-recycling processes.

In conclusion, the present study has led to the discovery of unique intermediate structures associated with vesicle-mediated secretion and membrane recycling in plant cells, and which do not

have any counterparts in animal cells. The reason for these unique membrane configurations appears to be that plant cells are under turgor pressure, and that this force affects both the integration of vesicle membrane into the plasma membrane and the return of excess plasma-membrane material to the cell interior.

Thanks are due to Drs. Stuart Craig, Donna Fernandez and Joel Stafstrom for thoughtful comments on the models and the manuscript. The excellent technical assistance of Carol Pefley and Marcia DeWit is gratefully acknowledged. Supported by National Institutes of Health grant GM 18639 to L.A.S.

References

- Aunis, D., Hesketh, J.E., Devillers, G. (1979) Freeze-fracture study of the chromaffin cell during exocytosis: Evidence for connections between the plasma membrane and secretory granules and for movements of plasma membrane-associated particles. *Cell Tissue Res.* **197**, 433–441
- Branton, D., Bullivant, S., Gilula, N.B., Karnovsky, M.J., Moor, H., Mühlethaler, K., Northcote, D.H., Packer, L., Satir, B., Satir, P., Speth, V., Staehelin, L.A., Steere, R.L., Weinstein, R.S. (1975) Freeze-etching nomenclature. *Science* **68**, 30–47
- Brown, M.S., Anderson, R.G.W., Goldstein, J.L. (1983) Recycling receptors: the round-trip itinerary of migrant membrane proteins. *Cell* **32**, 663–667
- Chandler, D.E., Heuser, J. (1980) Arrest of membrane fusion events in mast cells by quick freezing. *J. Cell Biol.* **86**, 666–674
- Chapman, R.L., Staehelin, L.A. (1986) Plasma membrane “rosettes” in carrot and sycamore suspension culture cells. *J. Ultrastruct. Res.* **93**, 87–91
- Chrispeels, M.J. (1983) The endoplasmic reticulum. In: *The biochemistry of plants*, vol. I: The plant cell, pp. 389–412, Tolbert, N.E., ed. Academic Press, New York
- Cram, W.J. (1980) Pinocytosis in plants. *New Phytol.* **84**, 1–17
- Craig, S., Staehelin, L.A. (1986) Structure of plant tissue frozen under high pressure. *J. Cell Biol.* **103**, 514a
- Farquhar, M.G. (1985) Progress in unraveling pathways of Golgi traffic. *Annu. Rev. Cell Biol.* **1**, 447–488
- Fernandez, D.E., Staehelin, A. (1985) Structural organization of ultrarapidly-frozen barely aleurone cells actively involved in secretion. *Planta* **165**, 455–468
- Fisher, G.W., Rebhun, L.I. (1983) Sea urchin egg cortical granule exocytosis is followed by a burst of membrane retrieval via uptake into coated vesicles. *Dev. Biol.* **99**, 456–472
- Gamborg, O.L. (1982) Callus and cell culture. In: *plant tissue culture methods*, pp. 1–9, Wetter, L.R., Constabel, E., eds. National Research Council of Canada, Saskatoon, Sask.
- Gilkey, J.C., Staehelin, L.A. (1986) Advances in ultrarapid freezing for the preservation of cellular ultrastructure. *J. Electronmicrosc.* **3**, 177–210
- Griffing, L.R., Mersey, B.G., Fowke, L.C. (1986) Cell-fractionation analysis of glucan synthase I and II distribution and polysaccharide secretion in soybean protoplast. *Planta* **167**, 175–182
- Helmkamp, G.M. (1986) Phospholipid transfer proteins: mechanism of action. *J. Bioenerg. Biomembr.* **18**, 71–91
- Hepler, P.K. (1981) The structure of the endoplasmic reticulum revealed by osmium tetroxide-potassium ferricyanide staining. *Eur. J. Cell Biol.* **26**, 102–110

- Hepler, P.K., Wayne, R.O. (1985) Calcium and plant development. *Annu. Rev. Plant Physiol.* **36**, 397–439
- Heuser, J.E., Reese, T.S., Dennis, M.S., Jan, Y., Jan, L., Evans, L. (1979) Synaptic vesicle exocytosis captured by quick freezing and correlated with quantal transmitter release. *J. Cell Biol.* **81**, 275–300
- Hübner, R., Depta, H., Robinson, D.G. (1985) Endocytosis in maize root cap cells. Evidence obtained using heavy metal salt solutions. *Protoplasma* **129**, 214–222
- Joachim, S., Robinson, D.G. (1984) Endocytosis of cationic ferritin by bean leaf protoplasts. *Eur. J. Cell Biol.* **34**, 212–216
- Kaplan, M.R., Simoni, R.D. (1985) Intracellular transport of phosphatidylcholine to the plasma membrane. *J. Cell Biol.* **101**, 441–445
- Kristen, U., Lockhausen, J. (1983) Estimation of Golgi membrane flow rates in ovary glands of *Aptenia cordifolia* using cytochalasin B. *Eur. J. Cell Biol.* **29**, 262–267
- Kroh, M., Knuiman, B. (1985) Exocytosis in non-plasmolysed and plasmolysed tobacco pollen tubes. *Planta* **166**, 287–299
- Lawson, D., Raff, M.C., Gomperts, B., Fewtrell, C., Gilula, N.B. (1977) Molecular events during membrane fusion. A study of exocytosis in rat peritoneal mast cells. *J. Cell Biol.* **72**, 242–259
- Lynch, D.V., Thompson, G.A. (1984) Retailored lipid molecular species: A tactical mechanism for modulating membrane properties. *Trends Biochem. Sci.* **9**, 442–445
- Mollenhauer, H.H., Morré, D.J. (1980) The Golgi apparatus. In: *The biochemistry of plants, vol. I: The plant cell*, pp. 438–483, Tolbert, N.E., ed. Academic Press, New York
- Morré, D.J., Kartenbeck, J., Franke, W.W. (1979) Membrane flow and interconversions among endomembranes. *Biochim. Biophys. Acta* **559**, 71–152
- Morré, D.J., Mollenhauer, H.H. (1983) Dictyosome polarity and membrane differentiation in outer cap cells of maize root tip. *Eur. J. Cell Biol.* **29**, 126–132
- Morris, M.R., Northcote, D.H. (1977) Influence of cations at the plasma membrane in controlling polysaccharide secretion from sycamore suspension cells. *Biochem. J.* **166**, 603–618
- Nakamura, S., Miki-Hiroshige, H. (1982) Coated vesicles and cell plate formation in the microspore mother cell. *J. Ultrastruct. Res.* **80**, 302–311
- Orci, L., Perrelet, A. (1978) Ultracellular aspects of exocytotic membrane fusion. In: *Membrane fusion*, pp. 629–656, Poste, G., Nicolson, G.L., eds. Elsevier/North Holland Biomedical Press, Amsterdam
- Orci, L., Perrelet, A., Friend, D.S. (1977) Freeze-fracture of membrane fusions during exocytosis in pancreatic B-cells. *J. Cell Biol.* **75**, 23–30
- Ornberg, R.L., Reese, T.S. (1981) Beginning of exocytosis captured by rapid-freezing of *Limulus* amoebocytes. *J. Cell Biol.* **90**, 40–54
- Palevitz, B.A., Hodge, L.D. (1984) The endoplasmic reticulum in the cortex of developing guard cells: Coordinate studies with chlorotetracycline and osmium ferricyanide. *Dev. Biol.* **101**, 147–159
- Picton, J.M., Steer, M.W. (1983) Membrane recycling and the control of secretory activity in pollen tubes. *J. Cell Sci.* **63**, 303–310
- Platt-Aloia, K.A., Thomson, W.W. (1982) Freeze-fracture of intact plant tissue. *Stain Technol.* **57**, 327–334
- Plattner, H. (1978) Fusion of cellular membranes. In: *Transport of macromolecules in cellular systems. Life Sciences Research Report II*, pp. 465–488, Silverstein, S.C., ed. Dahlem Konferenzen, Berlin
- Plattner, H. (1981) Membrane behavior during exocytosis. *Cell Biol. Int. Rep.* **5**, 435–459
- Robertson, J., Lyttleton, P. (1982) Coated and smooth vesicles in the biogenesis of cell walls, plasma membranes, infection threads and peribacteroid membranes in root hairs and nodules of white clover. *J. Cell Sci.* **58**, 63–78
- Robinson, D.G. (1984) *Plant membranes*. John Wiley & Sons, New York
- Robinson, D.G., Kristen, U. (1982) Membrane flow via the Golgi apparatus of higher plant cells. *Int. Rev. Cytol.* **77**, 89–127
- Sato, T. (1968) A modified method for lead staining of thin sections. *J. Electron. Microsc. (Tokyo)* **17**, 158–163
- Schekman, R. (1985) Protein localization and membrane traffic in yeast. *Annu. Rev. Cell Biol.* **1**, 115–143
- Schnepf, E. (1969) *Sekretion und Exkretion bei Pflanzen. Protoplasmatologia, vol. VIII*. Springer, Vienna New York
- Schnepf, E. (1974) Gland cells. In: *Dynamic aspects of plant ultrastructure*, pp. 331–357, Robards, A.W., ed. McGraw-Hill Publishers, London
- Schnepf, E., Busch, J. (1976) Morphology and kinetics of slime secretion in glands of *Mimulus tilingii*. *Z. Pflanzenphysiol.* **79**, 62–71
- Schmidt, W., Patzak, A., Lingg, G., Winkler, H. (1983) Membrane events in adrenal chromaffin cells during exocytosis: a freeze-etching analysis after rapid cryofixation. *Eur. J. Cell Biol.* **32**, 31–37
- Steinman, R.M., Mellman, I.S., Muller, W.A., Cohn, Z.A. (1983) Endocytosis and the recycling of plasma membrane. *J. Cell Biol.* **96**, 1–27
- Talmadge, K.W., Keegstra, K., Bauer, W.D., Albersheim, P. (1973) The structure of plant cell walls. I. The macromolecular components of the walls of suspension-cultured sycamore cells with detailed analysis of the pectic polysaccharides. *Plant Physiol.* **51**, 158–173
- Tanaka, T., Yamada, M. (1979) A phosphatidylcholine exchange protein isolated from germinated castor bean endosperms. *Plant Cell Physiol.* **20**, 533–542
- Tanchak, M.A., Griffing, L.R., Mersey, B.G., Fowke, L.C. (1984) Endocytosis of cationized ferritin by coated vesicles of soybean protoplasts. *Planta* **162**, 481–486
- Volkman, D. (1981) Structural differentiation of membranes involved in the secretion of polysaccharide slime by root cap cells of Cress (*Lepidium sativum* L.). *Planta* **151**, 180–188
- Volkman, D. (1984) The plasma membrane of growing root hairs is composed of zones of local differentiation. *Planta* **162**, 392–403